

SEISMIC RESPONSE ANALYSIS OF A COMMON DUCT AND INTERNAL PIPES

Kunihiko FUCHIDA*, Takashi AKIYOSHI**
 and Kenzou TOKI***

Analysis of seismic response of common ducts and internal pipes is presented here. A common duct is modeled as a uniform beam with a rectangular cross section and internal pipe as a rumped mass-spring system. First, based on the soil-common duct interaction to seismic waves, the axial and lateral responses of the common duct are analyzed. Then the internal pipe's response is investigated depending on the response of the common duct. Numerical computations are done mainly on the strains of the common duct and internal pipes. Results show that the common duct reduces the deformation of internal pipes, and the strain of the common duct concentrates at both ends in the case of large difference of motion between both ends structures and ground.

Keywords: common duct, seismic response, slippage, internal pipe, beam, elastic ground, wave propagation, interaction

1. INTRODUCTION

Recently construction of common ducts is stimulated in urban areas for the ease of maintenance of internal lifelines¹⁾. Thus much efforts are required for the investigations to reduce the disasters of the lifeline facilities for earthquakes and for the establishment of the reasonable guidelines for the aseismic design of common ducts⁹⁾.

So far with respect to the buried tubular structures, pipelines²⁾⁻⁵⁾ and tunnels⁶⁾⁻⁸⁾ have been investigated extensively. Especially analyses concerning buried pipelines for earthquakes seem to have put emphasis on the effect of propagation of earthquakes because of the thin structures.

In this paper we propose an analytical method of seismic response of the common ducts and internal pipes. The method to analyze the common ducts is based on our previous study¹¹⁾⁻¹³⁾ which treats the interaction between the soil and the buried pipes as that of uniform and continuous tubular structures. On the other hand, the internal pipes are analyzed as discretized methods since the input from the common duct is not uniform for those. Thus this gives rise for internal pipes to be analyzed independently of the common ducts for an earthquake propagating in an oblique direction.

2. GENERAL FORMULATION

In this study the following assumptions are

adopted :

- (1) Soil is linear, homogeneous and isotropic infinite medium.
- (2) Common duct is assumed to be a beam model with a rectangular cross section, with both ends connected to structures.
- (3) Earthquakes propagate within a horizontal plane.
- (4) The soil and the common duct are mutually interactive through the frictional interface¹¹⁾⁻¹³⁾.
- (5) The friction at the interface is assumed to be of Coulomb mechanism and linearized in terms of the slip displacement and the velocity amplitude (procedures are shown in the references¹¹⁾⁻¹³⁾).
- (6) Axial vibration and lateral one are independent each other.

2.1 Axial vibration of a common duct

When an earthquake P-wave propagates horizontally toward a common duct as shown in Fig.1, the governing equation for an axially vibrating common duct is written by¹¹⁾;

$$m_c \frac{\partial^2 v_{z1}}{\partial t^2} = E_c A_c \frac{\partial^2 v_{z1}}{\partial z^2} + p_{z1} \dots \dots \dots (1)$$

where v_{z1} = axial displacement of the common duct, m_c , E_c , A_c = unit length mass, Young's modulus and cross sectional area of the common duct, w_1 = displacement amplitude of incident P-wave, $p_{z1} = q_{z1} - k_{z1} \cdot v_{z1}$ = exerting axial force of soil to the unit length common duct in which q_{z1} is deduced from the reference 11 (p.26 Formulation of slippage) ;

$$q_{z1} = \frac{4\tau_s \left(\frac{1}{\mu k_l \sin \phi} + i \frac{l_0}{M_0} \right)}{S_0 + \frac{4\tau_s}{\pi} \left(\frac{1}{\mu k_l \sin \phi} + i \frac{l_0}{M_0} \right)}$$

* Assistant Professor, Dept. of Civil & Archi. Eng., Yatsushiro National College of Technology.

** D. Eng., Professor, Dept. of Civil & Envi. Eng., Kumamoto Univ.

*** D. Eng., Professor, Disas. Priv. Res. Inst., Kyoto Univ.

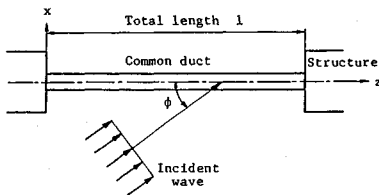


Fig.1 Geometry of a common duct model (Plan view)

$$\cdot (-l_0) \mu i k_l \sin \phi \cdot w_1 \cos \phi \cdot e^{i(\omega t - k_l z \cos \phi)},$$

τ_s = slip stress, S_0 = slip displacement amplitude, $M_0 = -m_c \omega^2 + E_c A_c k_l^2 \cos^2 \phi$, $k_{z1} = i l_0 \mu k_l \sin \phi$, ϕ = incident angle of P-wave to the axis of the common duct, l_0 = circumference length of the common duct, $k_l = (\omega/v_l)$ = wave number of P-wave, ω = circular frequency, $v_l = \sqrt{(\lambda + 2\mu)/\rho}$ = velocity of P-wave, λ, μ = Lamé's constants, ρ = mass density of soil. When slip occurs between common duct and soil, p_{z1} in eq. (1) becomes small.

Under steady-harmonic excitation, the solution of equation (1) is represented by the sum of the special solution $v_{z1}^{(1)}$ and the general solution $v_{z1}^{(2)}$ of the equation. Thus eliminating the time factor $e^{i\omega t}$ the solution takes the form

$$v_{z1} = v_{z1}^{(1)} + v_{z1}^{(2)} = H_{z1}(\omega) w_1 \cos \phi \cdot e^{-ik_{lz} \cos \phi} + A_1 e^{v_{z1} z} + A_2 e^{v_{z2} z} \dots \dots \dots (2)$$

where $H_{z1}(\omega)$ = axial frequency response function of the common duct⁽¹⁾;

$$H_{z1}(\omega) = \frac{k_{z1}}{k_{z1} - m\omega^2 + E_c A_c k_l^2 \cos^2 \phi} \dots \dots \dots (3)$$

A_1, A_2 = unknown coefficients,

$$v_1 = \sqrt{(k_{z1} - m\omega^2)/E_c A_c} = -v_2.$$

Now consider the following boundary conditions for the decision of unknown coefficients A_1, A_2 of equation (2);

$$\left. \begin{aligned} z = z_0; v_{z1} &= G_{z1}^{(0)}(\omega) w_1 \cos \phi e^{-ik_{lz_0} \cos \phi} \\ z = z_l; v_{z1} &= G_{z1}^{(l)}(\omega) w_1 \cos \phi e^{-ik_{lz_l} \cos \phi} \end{aligned} \right\} \dots \dots (4)$$

where $G_{z1}^{(0)}(\omega), G_{z1}^{(l)}(\omega)$ = axial frequency response functions of structures at both ends $z = z_0$ and z_l respectively.

Substituting equation (2) into equation (4), unknown coefficients A_1, A_2 are derived as follows;

$$A_1 = \frac{1}{e^{v_1(z_l - z_0)} - e^{-v_1(z_l - z_0)}} \cdot \left\{ - \left[G_{z1}^{(0)}(\omega) - H_{z1}(\omega) \right] \cdot w_1 \cos \phi e^{-ik_{lz_0} \cos \phi} e^{-v_1 z_0} + \left[G_{z1}^{(l)}(\omega) - H_{z1}(\omega) \right] \cdot w_1 \cos \phi e^{-ik_{lz_l} \cos \phi} e^{-v_1 z_l} \right\} \dots \dots \dots (5)$$

$$A_2 = \frac{1}{e^{v_1(z_l - z_0)} - e^{-v_1(z_l - z_0)}} \cdot \left\{ \left[G_{z1}^{(0)}(\omega) - H_{z1}(\omega) \right] w_1 \cos \phi e^{-ik_{lz_0} \cos \phi} e^{v_1 z_0} - \left[G_{z1}^{(l)}(\omega) - H_{z1}(\omega) \right] \cdot w_1 \cos \phi e^{-ik_{lz_l} \cos \phi} e^{v_1 z_l} \right\} \dots \dots \dots (5)$$

2.2 Lateral vibration of a common duct

Same procedures as the reference 11) will be applicable to the governing equation of a laterally vibrating common duct;

$$E_c I_c \frac{\partial^4 v_{x1}}{\partial z^4} + m_c \frac{\partial^2 v_{x1}}{\partial t^2} + \frac{\partial}{\partial z} \left(N_1 \frac{\partial v_{x1}}{\partial z} \right) = k_{x1} (w_1 \sin \phi e^{i(\omega t - k_{lz} \cos \phi)} - v_{x1}) \dots \dots \dots (6)$$

where v_{x1} = lateral displacement of the common duct, I_c = geometrical moment of inertia of the common duct, N_1 = axial force which is assumed to be independent of axial vibration(1), $k_{x1} = \rho A'_c \omega^2 h_s^2 K_x$ = lateral spring coefficient of ground for P-wave, A'_c = cross sectional area for common duct to occupy the soil space, $h_s^2 = 1 - (v_s/v_l)^2 \cos^2 \phi$, $v_s = \sqrt{\mu/\rho}$ = velocity of S-wave, $K_x = e^{q_1 B/2}$, $q_1 = (\omega/v_l) h_s$, B = width of cross section of common duct.

Now let $N_1 = E_c A_c (v_{z1}|_{z=z_1} - v_{z1}|_{z=z_0})/l$. Then the solution of equation (6) is represented by the sum of the special solution $v_{x1}^{(1)}$ and the general solution $v_{x1}^{(2)}$ of equation (7) in the same way as the axial case for steady harmonic excitation ;

$$v_{x1} = v_{x1}^{(1)} + v_{x1}^{(2)} = H_{x1}(\omega) w_1 \sin \phi e^{-ik_{lz} \cos \phi} + B_1 e^{\lambda_1 z} + B_2 e^{\lambda_2 z} + B_3 e^{-\lambda_1 z} + B_4 e^{-\lambda_2 z} \dots \dots \dots (7)$$

where, $H_{x1}(\omega)$ = lateral frequency response function of the common duct;

$$H_{x1}(\omega) = \frac{k_{x1}}{E_c I_c k_l^4 \cos^4 \phi - m\omega^2 - N_1 k_l^2 \cos^2 \phi + k_{x1}} \dots \dots \dots (8)$$

B_1, B_2, B_3, B_4 = unknown constant,

$$\lambda_1 = \sqrt{-\frac{N_1}{2 E_c I_c} + \sqrt{\left(\frac{N_1}{2 E_c I_c}\right)^2 - \frac{k_{x1} - m\omega^2}{E_c I_c}}}, \lambda_2 = \sqrt{-\frac{N_1}{2 E_c I_c} - \sqrt{\left(\frac{N_1}{2 E_c I_c}\right)^2 - \frac{k_{x1} - m\omega^2}{E_c I_c}}}, \dots \dots \dots (9)$$

Boundary conditions at both ends $z = z_0, z_l$ of the common duct are set for lateral displacements and bending moments;

$$z = z_0 \quad v_{x1} = G_{x1}^{(0)}(\omega) w_1 \sin \phi \cdot e^{-ik_{1z_0} \cos \phi}$$

$$M = k_r \left(\frac{\partial v_{x1}}{\partial z} \right)_{z=z_0} \\ = -E_c I_c \left(\frac{\partial^2 v_{x1}}{\partial z^2} \right)_{z=z_0}$$

$$z = z_1 \quad v_{x1} = G_{x1}^{(1)}(\omega) w_1 \cos \phi \cdot e^{-ik_{1z_1} \cos \phi}$$

$$M = k_r \left(\frac{\partial v_{x1}}{\partial z} \right)_{z=z_1} \\ = -E_c I_c \left(\frac{\partial^2 v_{x1}}{\partial z^2} \right)_{z=z_1} \dots \dots \dots (10)$$

where, $G_{x1}^{(0)}(\omega)$, $G_{x1}^{(1)}(\omega)$ = lateral frequency response functions of the structure at the both ends $z = z_0$, z_1 respectively, k_r = rotational spring coefficient at the connections between the common duct and the structures.

Adopting a similar process as in the previous section, the unknown coefficient B_1 , B_2 , B_3 , B_4 may be obtained as functions of displacement amplitude w_1 of input waves. Then the lateral displacement v_{x1} of equation (7) leads to the result ;

$$v_{x1} = w_1 \sin \phi [H_{x1}(\omega) e^{-ik_{1z_0} \cos \phi} + f_1(z)] \dots \dots \dots (11)$$

where $w_1 \sin \phi f_1(z) = B_1 e^{\lambda_1 z} + B_2 e^{\lambda_2 z} + B_3 e^{-\lambda_1 z} + B_4 e^{-\lambda_2 z}$.

For the case of the plane S-wave with the same incident angle as P-wave, axial and lateral displacements of common duct can be derived by replacing $w_1 \cos \phi$, $w_1 \sin \phi$ and $k_l = \omega/v_l$ with $w_2 \sin \phi$, $-w_2 \cos \phi$ and $k_s = \omega/v_s$ respectively in equations (7) and (11);

$$v_{z2} = v_{z2}^{(1)} + v_{z2}^{(2)} = H_{z2}(\omega) w_2 \sin \phi \cdot e^{-ik_{sz} \cos \phi} \\ + A_1 e^{\nu_1 z} + A_2 e^{\nu_2 z} \dots \dots \dots (12)$$

$$v_{x2} = (-w_2 \cos \phi) [H_{x2}(\omega) e^{-ik_{sz_0} \cos \phi} + f_2(z)] \dots \dots \dots (13)$$

where w_2 = displacement amplitude of S-wave, v_s = velocity of S-wave, $H_{z2}(\omega)$, $H_{x2}(\omega)$ = axial and lateral frequency response functions of the continuous common duct respectively.

2.3 Strain of a common duct

The axial strain ϵ_{a1} and bending strain ϵ_{b1} of the common duct for P-wave can be easily derived from the equations (7) and (11);

$$\epsilon_{a1} = \frac{\partial v_{z1}}{\partial z} = Z_{a1}(\omega) w_1 \dots \dots \dots (14)$$

$$\epsilon_{b1} = -\frac{B}{2} \frac{\partial^2 v_{x1}}{\partial z^2} = Z_{b1}(\omega) w_1 \dots \dots \dots (15)$$

where B = width of the common duct, $Z_{a1}(\omega)$, $Z_{b1}(\omega)$ = frequency response functions of axial and

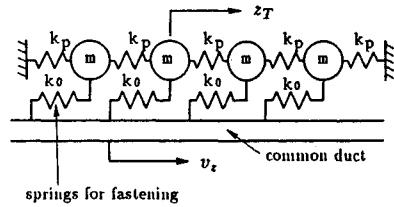


Fig.2 Geometry of discretized internal pipes in a common duct [the case for axial vibration]

bending strains of the common duct for P-wave, respectively, which lead to ;

$$Z_{a1}(\omega) = -ik_l \cos^2 \phi H_{z1}(\omega) e^{-ik_{1z} \cos \phi} \\ + \frac{\nu_1 \cos \phi}{e^{\nu_1(z_1-z_0)} - e^{-\nu_1(z_1-z_0)}} \\ \cdot \left\{ -[G_{z1}^{(0)}(\omega) - H_{z1}(\omega)] e^{-ik_{1z_0} \cos \phi} e^{\nu_1(z-z_1)} \right. \\ \left. + [G_{z1}^{(1)}(\omega) - H_{z1}(\omega)] e^{-ik_{1z_1} \cos \phi} e^{\nu_1(z-z_0)} \right\} \\ + \frac{-\nu_1 \cos \phi}{e^{\nu_1(z_1-z_0)} - e^{-\nu_1(z_1-z_0)}} \\ \cdot \left\{ [G_{z1}^{(0)}(\omega) - H_{z1}(\omega)] e^{-ik_{1z_0} \cos \phi} e^{\nu_1(z_1-z)} \right. \\ \left. - [G_{z1}^{(1)}(\omega) - H_{z1}(\omega)] e^{-ik_{1z_1} \cos \phi} e^{\nu_1(z_0-z)} \right\} \dots \dots \dots (16)$$

$$Z_{b1}(\omega) = -\frac{B}{2} \sin \phi \\ \cdot \left[-H_{x1}(\omega) k_l^2 \cos^2 \phi e^{-ik_{1z_1} \cos \phi} + f_1''(z) \right] \dots \dots \dots (17)$$

Therefore the total strain ϵ_1 of common duct for P-wave is represented by adding the axial strain ϵ_{a1} in equation (14) to the bending one ϵ_{b1} in equation (15);

$$\epsilon_1 = \epsilon_{a1} + \epsilon_{b1} = Z_1(\omega) w_1 e^{i\omega t} \dots \dots \dots (18)$$

where $Z_1(\omega) = Z_{a1}(\omega) + Z_{b1}(\omega)$.

In the same way the total strain ϵ_2 of the common duct for S-wave is written by ;

$$\epsilon_2 = \epsilon_{a2} + \epsilon_{b2} = Z_2(\omega) w_2 e^{i\omega t} \dots \dots \dots (19)$$

where ϵ_{a2} , ϵ_{b2} = axial and bending strains for S-wave respectively, $Z_2(\omega) = Z_{a2}(\omega) + Z_{b2}(\omega)$, $Z_{a2}(\omega)$, $Z_{b2}(\omega)$ = frequency response functions (FRF) of axial and bending strains of the common duct for S-wave, respectively.

2.4 Analysis of internal pipes

Let the internal pipes be uniformly discretized to masses and springs, and be elastically fastening to the common duct as in Fig.2. Then the solution of this system may be obtained by the sum of the static response $\{z_T\}$ and the dynamic response (devia-

tion) $\{Y(i\omega)\}$ of the pipes.

Static displacement $\{z_T\}$ can be written by

$$\{z_T\} = [K_z]^{-1} [K_{oz}] \{v_z\} \dots\dots\dots (20)$$

where, referring to the Fig.2, $[K_z]$ = stiffness matrix for pipes composed of elastic springs k_p and k_o which fastens pipes to the common duct, $[K_{oz}]$ = stiffness matrix with elastic springs k_o , $\{v_z\}$ = displacement vector of common duct.

Thus, neglecting the interaction between the common duct and internal pipes, the governing equation of the internal pipe is written by

$$[M] \{\ddot{y}\} + [K_z] \{y\} = - [M] [K_z]^{-1} [K_{oz}] \{\ddot{v}_z\} \dots\dots\dots (21)$$

where, $[M]$ = mass matrix, and $\{y\}$ = dynamic displacement vector of the internal pipes.

Using Fourier transform of equation (21), frequency response $\{Y(i\omega)\}$ of the pipe displacement is obtained ;

$$\{Y(i\omega)\} = \omega^2 [K_z - \omega^2 M]^{-1} \cdot [M] [K_z]^{-1} [K_{oz}] \{V_z(i\omega)\} \dots\dots\dots (22)$$

Total response displacement $\{Z(i\omega)\}$ of the pipe is finally given by adding the static displacement $z_T(t)$ in equation (20) to the dynamic displacement $Y(i\omega)$ in equation (22) ;

$$\{Z(i\omega)\} = \left\{ [K_z]^{-1} [K_{oz}] + \omega^2 [K_z - \omega^2 M]^{-1} \cdot [M] [K_z]^{-1} [K_{oz}] \right\} \{V_z(i\omega)\} \dots\dots\dots (23)$$

Thus the strains of the internal pipes are easily derived from equation (23) ;

$$\{\epsilon_{pa}(i\omega)\} = \left\{ [K_z]^{-1} [K_{oz}] + \omega^2 [K_z - \omega^2 M]^{-1} \cdot [M] [K_z]^{-1} [K_{oz}] \right\} \cdot \frac{\partial}{\partial z} \{V_z(i\omega)\} \dots\dots\dots (24)$$

$$\{\epsilon_{pb}(i\omega)\} = - \frac{B}{2} \left\{ [K_x]^{-1} [K_{ox}] + \omega^2 [K_x - \omega^2 M]^{-1} \cdot [M] [K_x]^{-1} [K_{ox}] \right\} \cdot \frac{\partial^2}{\partial z^2} \{V_x(i\omega)\} \dots\dots\dots (25)$$

where $\epsilon_{pa}(i\omega)$, $\epsilon_{pb}(i\omega)$ = axial and bending strains of the internal pipes.

Let Fourier transforms of input displacements of earthquakes be replaced w_1 , w_2 in eqs. (18) and (19), the frequency responses of common duct are obtained by using the equivalent method presented previously⁽¹¹⁾⁻⁽¹³⁾. In the same way, the responses of

Table 1 Boundary parameter g of end structure

	Axial (g_a)	Lateral (g_l)
Case 1	1.0	1.0
Case 2	0.5	1.0
Case 3	1.0	0.5

internal pipes are obtained from eqs. (24) and (25). Taking inverse Fourier transform of these equations, the strains of the common duct and the internal pipes can be obtained in time.

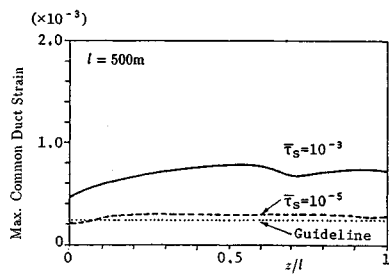
3. NUMERICAL RESULTS

3.1 Standard value of parameters

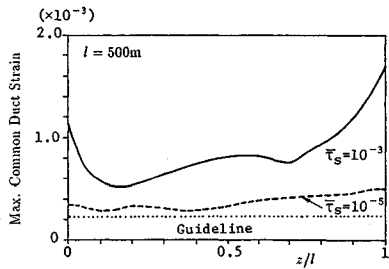
Numerical computations are conducted for the maximum response strain of common ducts and internal pipes for earthquakes. The standard values of the parameters of earthquakes, common duct, internal pipes and soils used for computations are as follows; incident angle of the input waves to the axis of common duct: $\phi = 45^\circ$, the shear wave velocity of soil : $v_s = 100$ m/s, ratio of P-to S-wave velocity : $v_l/v_s = 2.0$, ratio of frictional slip stress to shear modulus of soil : $\bar{\tau}_s = \tau_s/\mu = 10^{-3} \sim 10^{-5}$ (for example¹⁰⁾, $\bar{\tau}_s = 10^{-4}$ in the case of $\tau_s = 0.1$ kgf/cm², $\mu = 1000$ kgf/cm²), a referential length of the common duct : $D = B = h = 4.0$ m (width B , height h), nondimensional geometrical moment of inertia : $I_c/(A_c \cdot (D/2)^2) = 0.67$, total length of the common duct : $l = 100 \sim 500$ m, equivalent wave velocity of the common duct : $v_{cp} = 1000$ m/s, nondimensional mass ratio : $\bar{m} = m/\rho B h = 0.5$ (ρ = mass density of soil), ratio of rotational spring constant to bending stiffness at the connection between the common duct and structures : $k_r/E_c I_c = 1.0$ (m⁻¹), axial spring constant of the pipe : $k_{pz} = E_p A_p/l_p = 3 \times 10^4$ tonf/m (Young's modulus of pipe : $E_p = 1.5 \times 10^7$ tonf/m², cross sectional area of pipe : $A_p = 0.01$ m², pipe length : $l_p = 5$ m), bending spring constant of the pipe : $k_{px} = 3 \times 10^4$ tonf/m, spring constant between internal pipe and common duct : $k_p^* = 3 \times 10^4$ tonf/m. NS and EW components of El Centro earthquakes (1940) are used as the input P- and S-waves respectively with the maximum amplitude of 100 gal.

In this paper the boundary conditions are defined by frequency response functions of the structures at both ends $G_{z1}^{(i)}(\omega)$, $G_{z1}^{(l)}(\omega)$ in eqs. (4) and (10). Now define frequency-independent boundary parameter $g_a = G_{z1}^{(i)}(\omega)$, $g_l = G_{z1}^{(l)}(\omega)$ in which g_a and g_l are the axial and lateral cases respectively. Thus $1 - g_a$ or $1 - g_l$ mean the degree of difference of motion between the structures at both ends of the common duct and the ground.

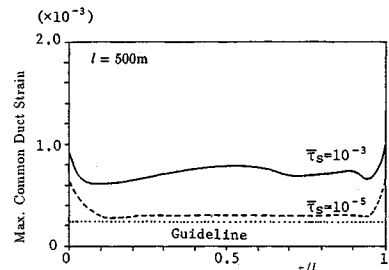
In the analysis three cases of boundary parameter g are assumed as shown in table 1. Case 1 ($g = 1$) means that both ends of common duct follow



(a) Case 1 ($g_a = g_t = 1.0$)

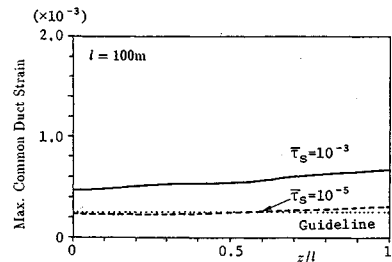


(b) Case 2 ($g_a = 0.5, g_t = 1.0$)

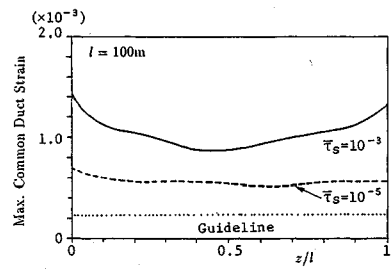


(c) Case 3 ($g_a = 1.0, g_t = 0.5$)

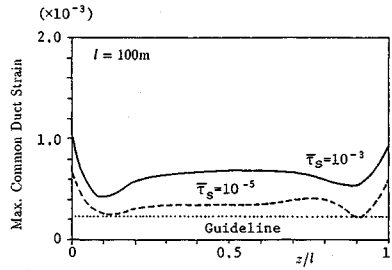
Fig. 3 Distribution of maximum common duct strain ($l = 500$ m)



(a) Case 1 ($g_a = g_t = 1.0$)



(b) Case 2 ($g_a = 0.5, g_t = 1.0$)



(c) Case 3 ($g_a = 1.0, g_t = 0.5$)

Fig. 4 Distribution of maximum common duct strain ($l = 100$ m)

completely the surrounding ground movement. However in Case 2 and 3 ($g=0.5$), implies that 50% of difference of motion between the structure and the ground may be occurred in the axial or lateral-directional-vibration.

3.2 Strain of the common duct

Fig.3 gives the graphs of axial distribution of maximum response strains of the common duct of the length $l=500$ m in which (a), (b) and (c) represent Case 1, Case 2 and Case 3 in Tabel 1, respectively. Fig.3 (a) shows that the strain of the common duct distributes almost uniformly along the axis for $\bar{\tau}_s=10^{-3}$ (:solid line), but decreases for small $\bar{\tau}_s$ of $\bar{\tau}_s=10^{-5}$ (:broken line). This is due to the relaxation of axial strain by slippage. For Fig.3 (b) and (c) which are the cases of 50% difference ($1-g$) between the structure and the ground in the direction of axial or lateral respectively, the difference ($1-g$) increases strains at both ends but slippage (: broken lines) also decreases the strain of the common duct. For the sake of comparison, the strain of the common duct computed by the

conventional guidelines for seismic design of common duct is also shown in Fig.3 as a dotted line. At present the aseismic design of a common duct depends on the guideline for the seismic design of pipelines. Therefore, following the conventional design procedure for the common duct considered, the strain may be computed for the natural period of surface layer of 1.0 sec and the input amplitude of 100 gal. This natural period 1.0 sec is closed to predominant period of El Centro earthquake. It is noted that the response strain by the guidelines are comparable for the strain by proposed method under the slip conditions ($\bar{\tau}_s = 10^{-5}$) and, the strain by proposed method at both ends are larger than the guidelines for the case of large difference ($1-g$) as in Fig.3 (b), (c) (Cases 2, 3).

Fig.4 also shows the distribution of the strain of relatively short-length common duct ($l=100$ m). General trend of distribution as in Fig.4 is similar to that in Fig.3, implying that the length is not a key parameter for the design of a common duct.

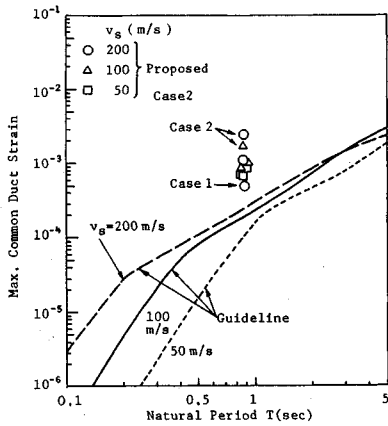


Fig. 5 Maximum strain of a common duct versus natural period of surface layer

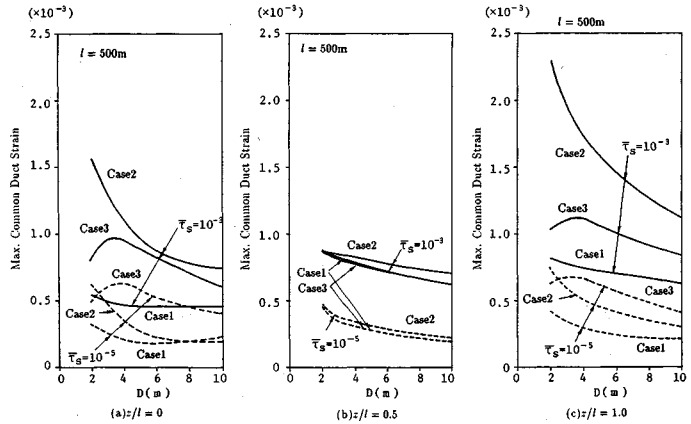


Fig. 6 Maximum strain versus side length D of the common duct

For another comparison the strains computed by the proposed method and the guidelines are plotted against the natural period of the surface layer, in Fig. 5. As the natural period increases, the strain given by the guidelines increases. In the diagram the strains of the common duct by the proposed method are also plotted for various S-wave velocities, v_s and three cases of boundary parameter, g . These values are larger than the values computed as for guidelines at the natural period of 0.85 sec, and that in the case 2 of large difference $1 - g$ (50%) at end structures extremely exceeds that of the latter. In the guideline the common duct is assumed to extend infinitely, but in the proposed method its length to be finite. Thus it may be difficult to compare the proposed method with the guideline directly.

Fig. 6 shows maximum strain of the common duct at both ends ($z/l=0.0$ and 1.0) and the center ($z/l=0.5$) versus the referential length D ($=$ width B = height h) of the cross section of the common duct. The strain concentration at both ends of the common duct decreases with increasing D or the cross-sectional area. This is a scale effect that a large-scaled rigid structure induces an input energy loss. As shown in the case of Figs. 3 and 4, slippage for small τ_s releases the concentrated strains at the ends of the common duct. However, small-cross-sectional common duct (small D) induces high strain concentration at the ends, especially for the case of a large axial difference $1 - g$ (:Case 2).

Since the solution in this study such as eq.(11) includes the coordinate z_0 the response is dependent on z_0 . Then the response of common duct has the error due to the imperfect solution. Fig. 7 shows the existing range (:hatched) of the response strain of the common duct with changing z_0 from $-l/2$ to $l/2$, and (a), (b) and (c) in Fig. 7 denote same

correspondences as in Figs. 3, 4. The degree of dependence of the strain on the coordinate z_0 is small at the middle part ($0.1 < z/l < 0.9$) of the duct, but large at the ends of the duct especially for Case 2.

3.3 Strain of internal pipes

Fig. 8 shows the distribution of response strain of the common duct and internal pipes under the soil condition $\bar{\tau}_s = 10^{-3}$ by broken and solid lines respectively, in which (a), (b) and (c) correspond to Cases 1, 2 and 3 respectively. By and large the strain distribution of the pipe are similar to and far less than that of the common duct. Thus the pipes are protected properly from seismic forces by the common duct. For the case of no difference $1 - g$ between soil-structure [Fig. 8 (a)], the strains of pipes fastened to the common duct distribute uniformly. Even for the case of large difference $1 - g$ [Fig. 8 (b) and (c)], the strain concentration of the pipe is not so remarkable as the common duct at both ends.

Fig. 9 shows the effect of the stiffness of fastening springs k_o on the maximum response strain of pipes in the common duct in which (a), (b) and (c) denote the same boundary condition as in Fig. 3 and 4. For any case, tight fastening ($k_o = k_o^* \times 10$; k_o^* = reference spring constant for fastening) increases the pipe strain due to little input loss from the common duct. Therefore loose fastening of inner pipes to the common duct is desirable for the protection against the excitation by the common duct.

Fig. 10 is the plots of maximum pipe strain at both ends of the common duct ($z/l=0.0$ and 1.0) versus ratio of fastening spring constant k_o to the standard one k_o^* . As for the case of Fig. 9, it can be noted that loose fastening of internal pipes to the common duct is effective for lowering the strains.

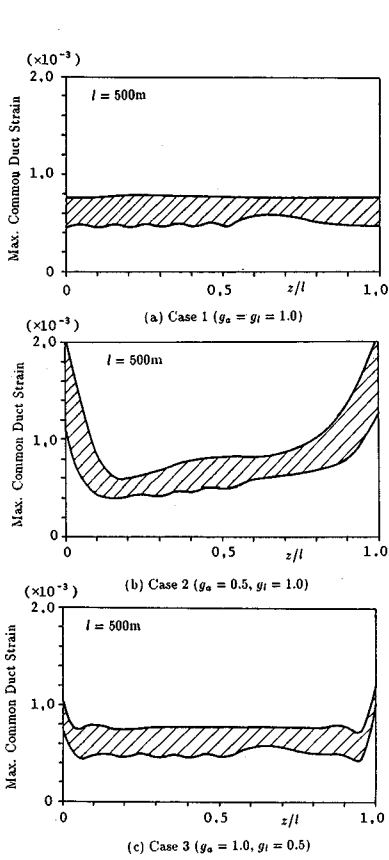


Fig. 7 Dependence of maximum common duct strains on the coordinate z_0

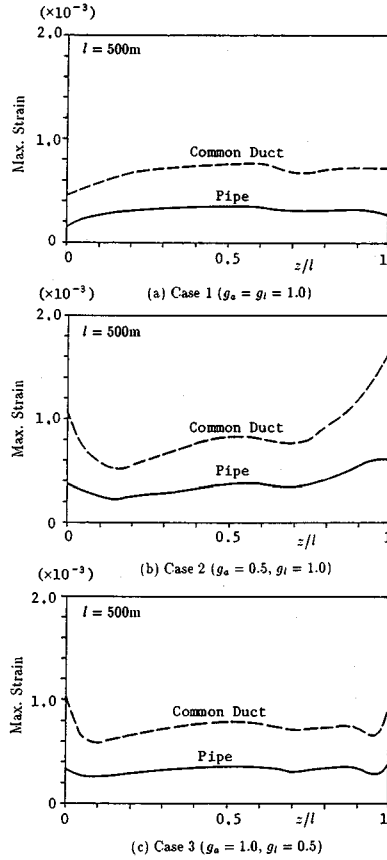


Fig. 8 Distribution of maximum pipe and common duct strain

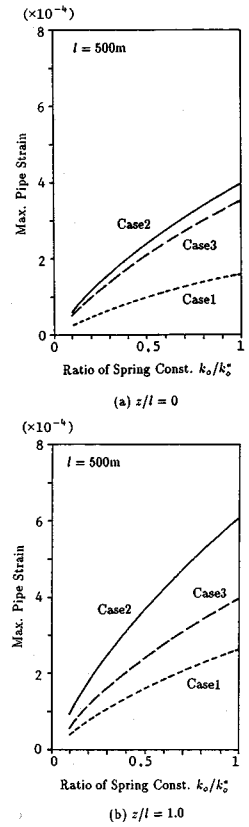


Fig. 10 Maximum pipe strain in common duct versus stiffness of fastening spring

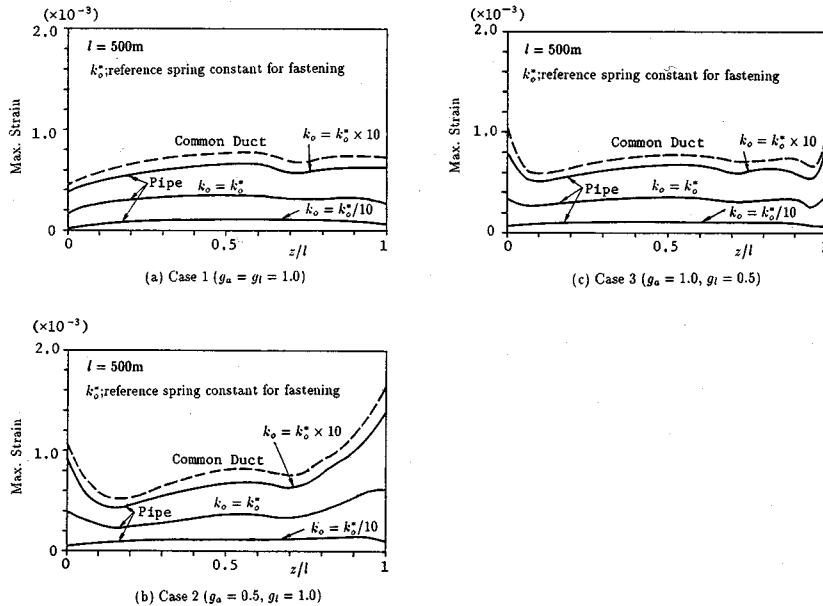


Fig. 9 Effect of the stiffness of fastening spring on the maximum pipe strain in common duct

4. CONCLUSIONS

In this paper the seismic responses of a common duct and internal pipes are analyzed approximately by considering the common duct as a uniform beam and the internal pipe as rumped masses and springs. The strain behavior of the common duct and the internal pipes subjected to seismic waves are mainly investigated due to the higher priority for the design of underground linear structures. Results obtained are summarized as follows:

- (1) Strain concentration which arises at the joints between structures and common duct is induced strongly by the axial difference between the ground and the structures at both ends of the common duct.
- (2) Slippage affects for lowering the strain of the common duct and the internal pipes.
- (3) Large-scaled cross section is advantageous for lowering the strain of the common duct but the length is not a key parameter for small strain.
- (4) Loose-fastening of inner pipes to the common duct induces not only lowering the strain of pipes but also releasing the concentrated strains at the duct-structure joints.

REFERENCES

- 1) Sato, H.: Common Duct, Morikita Shuppan, pp.1-82, 1981 (in Japanese)
- 2) Toki, K. and Takada, S.: Earthquake Response Analysis of Underground Tubular Structure, Bull. Disas. Prev. Res. Inst., Kyoto Univ., Vol.24, Part 2, No.221, pp.107-125, 1974.
- 3) Shinozuka, M. and Koike, T.: Estimation of Structural Strains in Underground Lifeline Pipes, Lifel. Earthq. Eng.-Buried Pipel., Seism. Risk, and Instrum., ASME, pp.31-48, 1979.
- 4) Takada, S.: Seismic Response Analysis of Buried PVC and Ductile Iron Pipelines, Proc. Pressure Vessel and Piping Conf., ASME, pp.23-32, 1980.
- 5) Nishio, N. and Satake, M.: Characteristics of Deformation in a Buried Pipeline under Sinusoidal Ground Motion, Natural Disaster Science, Vol.5, No.1, pp.53-68, 1983.
- 6) Kuribayashi, E., Kawashima, K. and Shibata, M.: Seismic Response Analysis of Cross Sectional Force and Displacement along Submerged Tunnel, Technical Memorandum of Public Works Research Institute, Ministry of Construction, Vol.1193, pp.1-37, 1985. (in Japanese)
- 7) Suzuki, T., Tamura, C. and Maeda, H.: Earthquake Observation and Response Analysis of Shield Tunnel, Proc. 7th Japan Earthquake Engineering Symposium, pp.1903-1908, 1986.
- 8) Ikeda, N., Kato, K. and Hagihara, M.: Study on Seismic Behavior of Reinforced Concrete Immersed Tunnels Having Flexible Joint, Proc. JSCE., No.402/V-10, pp.71-80, 1989. (in Japanese)
- 9) Japan Road Association: The Guideline for Design of Common Duct, 1986 (in Japanese).
- 10) Japan Gas Association: Guideline for Seismic Design of Gas Pipeline, 1982 (in Japanese).
- 11) Akiyoshi, T. and Fuchida K.: Effect of Slippage on the Seismic Response of Buried Pipes, Proc. of JSCE, No.334, pp.25-34, 1983. (in Japanese)
- 12) Akiyoshi, T. and Fuchida K.: Soil-Pipeline Interaction Through a Frictional Interface During Earthquakes, Soil Dynamics and Earthquake Engineering, Vol.3, No.1, pp.27-34, 1984.
- 13) Akiyoshi, T. and Fuchida K.: An Approximate Solution of Earthquake-Induced Slippage of Structures on/in Soil, Proc. of 9 WCEE, Vol.3, pp.447-452, 1988.

(Received January 12:1990)

共同溝および内部管路の地震応答解析

淵田邦彦・秋吉 卓・土岐憲三

地震時の都市機能維持のため共同溝の耐震性の問題は重要と考えられる。本論文では、すべりを考慮した波動解より地盤ばねを定義し、共同溝を弾性床上のはりとし、不規則波に対する軸および曲げひずみ応答を解析した。さらに内部管路を集中質量系の離散モデルに置き換えた解析も行った。数値計算の結果、ひずみ応答の端部への集中や内部管路が共同溝により保護されることなどを明らかにし、また現行の設計指針との比較も行っている。